Day, R. A. (1999). *Géotechnique* **49**, No. 2, 231–245

Net pressure analysis of cantilever sheet pile walls

R. A. DAY*

There are many methods for the analysis and design of embedded cantilever retaining walls. They involve various different simplifications of the net pressure distribution to allow calculation of the critical retained height. In the UK, it is commonly assumed that net pressure consists of the sum of the active and passive limiting pressure values. In the USA, the net pressure is commonly simplified by a three-line rectilinear pressure distribution. Recently, centrifuge tests have led to a proposed semi-empirical rectilinear method in which an empirical constant defines the point of zero net pressure. Finite element analyses presented in this paper examine the net pressure distribution at limiting equilibrium. The study shows that the point of zero net pressure for a best-fit rectilinear approximation is dependent on the ratio between the passive and active earth pressure distributions at limiting conditions. A simple empirical equation is proposed which defines the point of zero pressure. The predictions for the critical retained height and bending moment distribution using this empirical equation are in excellent agreement with the finite element results and centrifuge data. They are in better agreement than the predictions of the commonly used analysis methods.

KEYWORDS: earth pressure; retaining walls; sheet piles.

Il existe plusieurs méthodes pour analyser et concevoir des murs de soutènement en porte-à-faux enfouis dans le sol. Ces méthodes passent par diverses simplifications de la distribution de pression nette pour permettre le calcul de la hauteur critique retenue. Au Royaume-Uni, on assume communément que la pression nette est constituée de la somme des valeurs de pression limites actives et passives. Aux USA, la pression nette est communément simplifiée par une distribution rectiligne de la pression sur trois lignes. Récemment, des essais centrifuges ont conduit à proposer une méthode recitligne semi empirique dans laquelle une constante empirique définit le point zéro de pression nette. Les analyses d'éléments finis présentées dans cet exposé examinent la distribution de pression nette au point d'équilibre limite. Cette étude montre que le point zéro de pression nette permettant d'obtenir l'approximation rectiligne qui convient le mieux, dépend du rapport entre les distributions de pressions terrestres actives et passives en conditions limites. Nous proposons une équation empirique simple qui définit le point de pression zéro. Les prévisions pour la hauteur critique retenue et la distribution du couple de flexion qui font appel à cette équation empirique montrent un excellent accord avec les résultats des analyses d'éléments finis et les données centrifuges. Elles sont plus cohérentes que les prédictions obtenues par les méthodes d'analyse couramment employées.

INTRODUCTION

A cantilever sheet pile retaining wall consists of a vertical structural element embedded in the ground below the retained material. The upper part of the wall provides a retaining force due to the wall stiffness and the embedment of the lower part. The embedded cantilever wall obtains its ability to resist the pressure of the retained soil by developing resisting earth pressures on the embedded portion of the wall. Embedded cantilever sheet pile retaining walls are frequently used for temporary and permanent support of excavations up to about 4·5 m high.

The distribution of earth presure on the embedded part of the wall is dependent on the complex interaction between the wall movement and the ground. Many methods for analysis and design of embedded cantilever walls have been proposed and these have been reviewed by Bica & Clayton (1989). Each method makes various assumptions concerning the distribution of earth pressure on the wall and the deflection or wall movement. Most of the methods are limit equilibrium methods based on the classical limiting earth pressure distributions. Model studies on embedded walls have been performed by Rowe (1951), Bransby & Milligan

Manuscript received 3 February 1998; revised manuscript accepted 9 September 1998.
Discussion on this paper closes 2 July 1999; for further details see p. ii.

* University of Queensland.

(1975) and Lyndon & Pearson (1985). Bica & Clayton (1993) have produced some empirical charts for the design of cantilever walls.

King (1995) suggested an analytical limit equilibrium approach for dry cohesionless soil, involving different assumptions from the previous methods. One of King's assumptions involves an empirically determined parameter. King makes a recommendation, based on the results of centrifuge test results, for an appropriate value of the empirical parameter.

This paper compares King's proposal with two other cantilever wall design methods commonly used in practice in the UK and the USA. In particular, this paper examines the value that King suggested for the empirical parameter. A series of finite element analyses of embedded cantilever walls in dry cohesionless soil have been performed to add further data to allow the appropriate selection of the value of this parameter. A new recommendation is made, based on the finite element results and other experimental data.

COMMON ANALYSIS METHODS

The basis of the limit equilibrium methods is the prediction of the maximum height of excavation for which static equilibrium is maintained. This is known as the limiting equilibrium situation. It is therefore important to be able to accurately evaluate the earth pressure acting on each side of the wall in the limiting equilibrium condition.

The actual distribution and magnitude of earth pressure on an embedded retaining wall is dependent on the complex interaction of the wall and the soil. The general shape of the earth pressure distribution is shown in Fig. 1. The common limit equilibrium design and analysis methods are all based on this general shape. Each method makes different simplifications and assumptions that modify the general shape of the pressure distribution to enable a solution to be found. These are discussed below.

UK method

In this method, the earth pressure distribution is simplified as shown in Fig. 2. The lines marked K_a and K_p indicate the active and passive limiting earth pressure values defined by the earth pressure coefficients K_a and K_p. The force R, representing the net force acting below the point O, is assumed to act at point O. Moment equilibrium about O yields the value d_0 required for stability. The penetration depth, d, is then taken as $d = 1{\cdot}2d_0$. Finally, a check is made to ensure that the force R can be mobilized on the wall below point O. The bending moment diagram is calculated from the assumed pressure distribution. This method is commonly used in the UK. It is described by Padfield & Mair (1984).

The limiting equilibrium condition is defined as the situation in which the depth of penetration, d, is just sufficient to maintain equilibrium for a retained height, h. This condition may also be called the failure or critical condition. It is useful to define the height h in the non-dimensional form $h' = h/d$. The limiting equilibrium or critical value of h' given by the UK method is:

$$h'_c = \frac{\sqrt[3]{(K_p/K_a)} - 1}{1{\cdot}2} \tag{1}$$

Five methods are used in design to incorporate a factor of safety against collapse. These involve increasing the embedment depth (F_d), reducing the strength parameters (F_s), reducing the passive pressure coefficient (F_p), reducing the net passive pressure (F_{np}), or reducing the net available passive pressure (F_r) (Padfield & Mair, 1984).

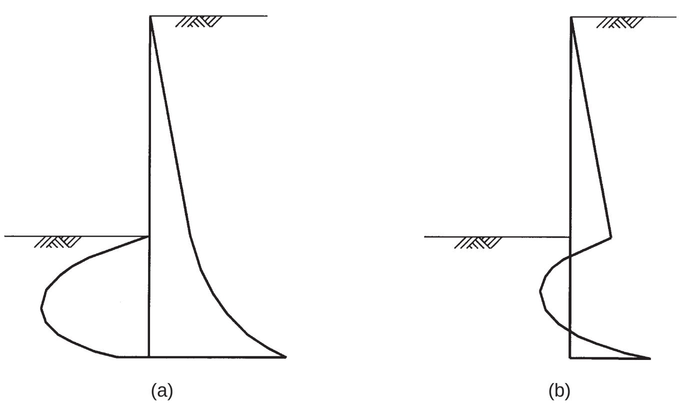

Fig. 1. Net pressure on embedded cantilever wall: (a) pressure distribution; (b) net pressure

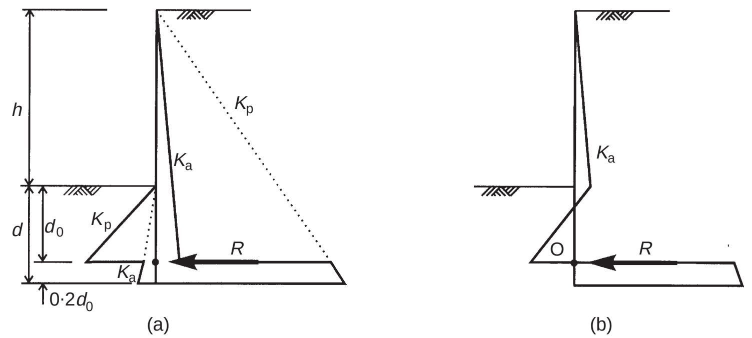

Fig. 2. Simplified pressure distribution – UK method: (a) pressure distribution; (b) net pressure

USA method

In this method, the earth pressure distribution is simplified by the rectilinear distribution shown in Fig. 3. The rectilinear distribution is characterized by the parameters p_a, p_1, p_2 and y. This is a modern version of a method initially proposed by Krey in 1932. It is described by Bowles (1988) and King (1995). This method is commonly used in the USA.

For a given retained height, h, it is required to determine the minimum depth of penetration and the corresponding pressure distribution that just maintains stability – the limiting equilibrium solution. In this situation, it is reasonable to assume that the pressure behind the wall at the dredge level, p_a, is equal to the active pressure limit. Hence, there are four unknown values, d, p_1, p_2 and y, which need to be determined.

The consideration of horizontal force and moment equilibrium provides two equations. In order to obtain a solution, two more assumptions are necessary. In the USA method these assumptions are as follows:

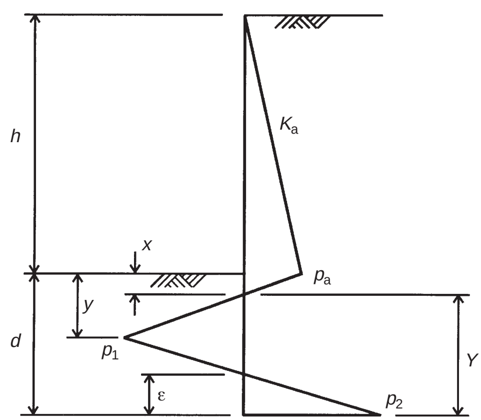

Fig. 3. Rectilinear pressure distribution

(*a*) The limiting passive pressure is fully mobilized on the wall immediately below dredge level. This assumption gives the gradient of the rectilinear pressure distribution between p_a and p_1. It is equal to the passive pressure gradient minus the active pressure gradient, $\gamma(K_p - K_a)$, where γ is the bulk unit weight of the soil.

(*b*) The value of p_2 is equal to the passive pressure limit on the retained side minus the active pressure on the dredged side (equation (2)). This is the maximum possible value which p_2 can have:

$$p_2 = \gamma(h + d)K_p - \gamma d K_a \tag{2}$$

The equations of equilibrium and the constraints imposed by the two assumptions yield equation (3) (King, 1995). For a given value of h, this equation can be solved for Y and hence the limiting equilibrium depth of penetration d, and h'_c:

$$Y^4 + \left(\frac{q}{m}\right)Y^3 - \left(\frac{8P}{m}\right)Y^2 - \frac{6P}{m^2}(2mb + q)Y - \frac{P}{m^2}(6bq + 4P) = 0 \tag{3}$$

where

$$q = K_p\gamma(h + x) - K_a\gamma x; \quad m = (K_p - K_a)\gamma$$
$$b = \frac{(h + 2x)}{3}; \quad x = \frac{K_a\gamma h}{m} \tag{4}$$
$$P = \tfrac{1}{2}K_a\gamma h(h + x)$$

Two methods are used in design to incorporate a factor of safety against collapse. Either the embedment depth is increased by 30% or a factor of safety is used to reduce the passive pressure coefficient.

GENERAL RECTILINEAR NET PRESSURE METHOD

This method proposed by King (1995) is similar to the USA method. The earth pressure is simplified by a similar rectilinear net pressure distribution (Fig. 3). Force and moment equilibrium and the first of the assumptions made in the USA method provide three equations or conditions. The general rectilinear net pressure method differs from the USA method only in the second assumption required to obtain a solution. The second assumption involves the location of the point, near the bottom of the wall, of zero net pressure. King (1995) suggested that the assumption $\varepsilon' = \varepsilon/d = 0{\cdot}35$ (Fig. 3) provided good predictions of failure height and bending moment distribution. This recommendation was based on the results of centrifuge tests. The advantage of this method is that the value of p_2 is not prescribed as being equal to its maximum possible value.

Application of the general rectilinear method

Force and moment equilibrium yield the following two equations (King, 1995):

$$x' = \frac{y'[(1-2\varepsilon') - y'(1-\varepsilon')]}{h'(1-\varepsilon'-y') - y'^2 + (1-2\varepsilon')} \qquad (5)$$

and

$$[(1-\varepsilon')h' + (1-2\varepsilon')]y'^2 + [(1-\varepsilon')h'^2 - (1-3\varepsilon')]y' - [(1-2\varepsilon')h'^2 + (1-3\varepsilon')h'] = 0 \qquad (6)$$

where $x' = x/d$, $h' = h/d$, $y' = y/d$, and $\varepsilon' = \varepsilon/d$.

Thus for a given value of h' and an assumed value of ε', the values of y' and x' can be determined from equations (5) and (6). The rectilinear pressure distribution is then fully defined in terms of the non-dimensional parameters x', y' and ε'. However, the depth of embedment, d, remains unknown. It is interesting to note that equations (5) and (6) are dependent only on the geometrical parameters. They are independent of the soil density and the active and passive pressure coefficients K_a and K_p.

The first assumption of the rectilinear pressure distribution defines the distance x (Fig. 3) at limiting equilibrium:

$$\frac{x}{p_a} = \frac{1}{\gamma(K_p - K_a)} \qquad (7)$$

where, $p_a = \gamma h K_a$

The limiting equilibrium or failure criteria can therefore be expressed in the form (King, 1995)

$$\left(\frac{x}{h}\right)_c = \left(\frac{x'}{h'}\right)_c = \frac{1}{K_p/K_a - 1} \qquad (8)$$

Using equations (5) and (6), the relationship between x'/h' and h' can be calculated for different values of ε' (Fig. 4). For a particular situation (K_a and K_p given by soil strength and wall friction angles), the critical value of h' can therefore be determined using Fig. 4 and equation (8) with the assumed value of ε'.

EXAMINATION OF THE METHODS

General rectilinear net pressure method

From Fig. 4 it can be seen that for the larger values of ε' there is a maximum value of x/h. In

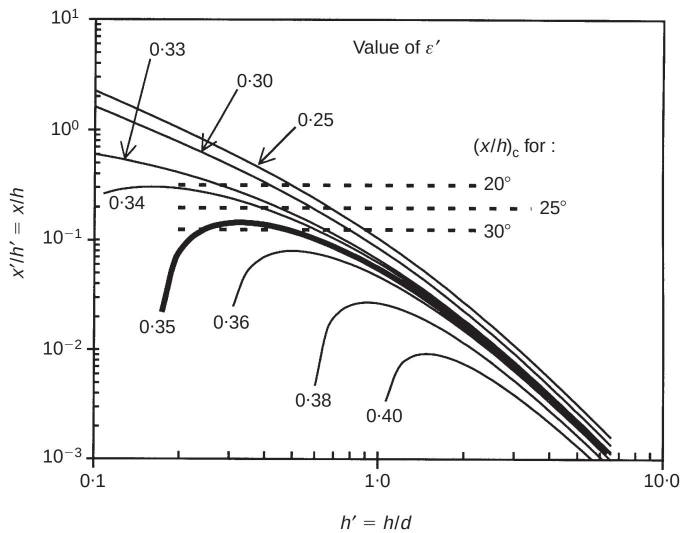

Fig. 4. Relationship between x/h and h'

fact, if ε' is greater than 1/3, there exists a maximum value for x/h (not shown on figure). If the critical value of x/h given by equation (8) is greater than this maximum, then a solution which satisfies the equations of equilibrium and the assumed value of ε' does not exist. Fig. 4 also illustrates that if the critical value of x/h is less than the maximum value, there are two valid solutions for h' which satisfy the assumptions, the larger value being of practical interest.

The critical values of x/h calculated from equation (8) for the case of a frictionless wall are shown in Fig. 4 for $\phi' = 20°$, 25° and 30°. For these cases, $K_p/K_a = 4{\cdot}2$, 6·1 and 9·0 respectively. The recommendation of King, that ε' is assumed constant and equal to 0·35, does not yield a solution if K_p/K_a is less than 7·90 (e.g. frictionless walls in low-strength soils). In practice, however, a solution is possible.

Clearly, this is a deficiency. It would appear that, for situations with lower values of K_p/K_a, the value of ε' at limiting equilibrium is less than 0·35.

Failure depth of excavation

Equations (1) and (8) indicate that the critical retained height h_c' is dependent only on the ratio K_p/K_a. The variation of h_c' calculated using each method is plotted in Fig. 5 for a range of values of K_p/K_a. The range of possible values of K_p/K_a is very large. For a frictionless wall in a $\phi' = 20°$ material, $K_p/K_a = 4{\cdot}2$, and for a rough wall in a $\phi' = 50°$ material, $K_p/K_a = 477$. The critical values predicted by the rectilinear net pressure method are plotted for a range of assumed values of ε'.

Figure 5 highlights the following interesting points:

(*a*) The UK and USA methods predict values that lie on lines nearly parallel to lines of constant ε'.
(*b*) The UK method is very close over the whole range of K_p/K_a to the rectilinear net pressure method if a value of $\varepsilon' = 0{\cdot}27$ is assumed.
(*c*) The assumptions of the USA method yield a value of ε' that varies between about 0·1 at high values of K_p/K_a and 0·15 at low values (see also Fig. 18).
(*d*) King's recommendation of $\varepsilon' = 0{\cdot}35$ is more conservative than both the UK and the USA methods.

FINITE ELEMENT ANALYSES

A series of two-dimensional plane strain finite element analyses have been performed to determine the pressure distribution on an embedded cantilever wall at limiting equilibrium for comparison with that assumed in the limit equilibrium methods described above. In the finite element analyses, the limiting equilibrium height of excavation was determined by 'excavating' elements from the mesh in front of a 10 m deep wall until numerical convergence was not achieved. Details of the mesh and boundary conditions are shown in Fig. 6. The displacement of the top of the wall is plotted against the excavation depth in Fig. 7. This plot is necessary to ensure that the failure to converge was indeed due to a physical instability of the wall, rather than a numerical problem. Before excavation began, the initial horizontal stress in the soil was equal to half the vertical

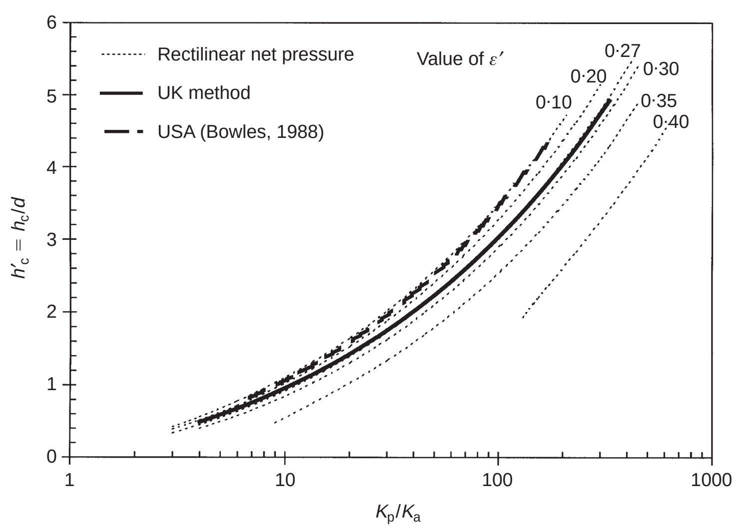

Fig. 5. Critical height of excavation

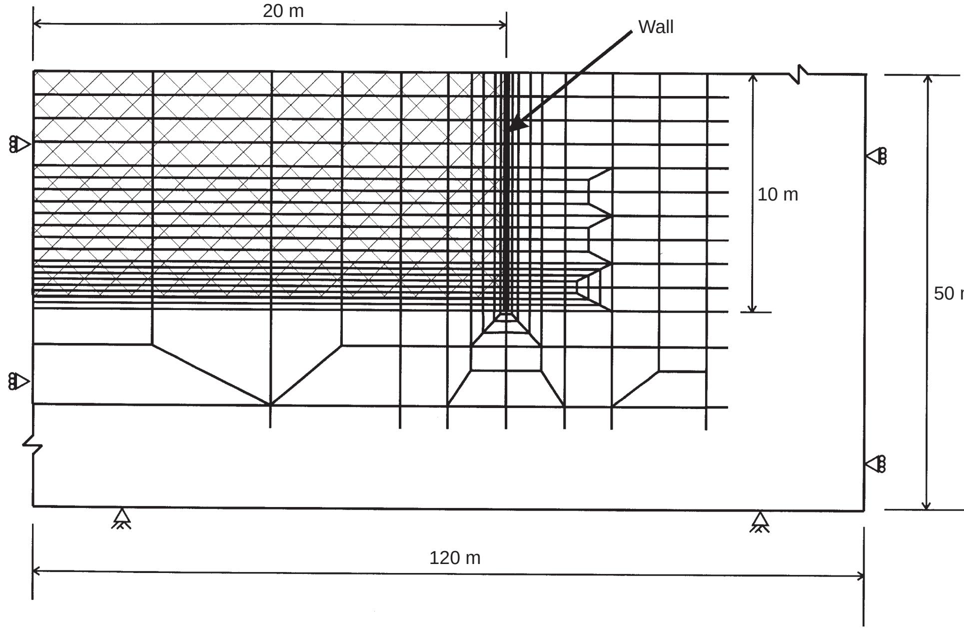

Fig. 6. Finite element mesh – excavated elements cross-hatched

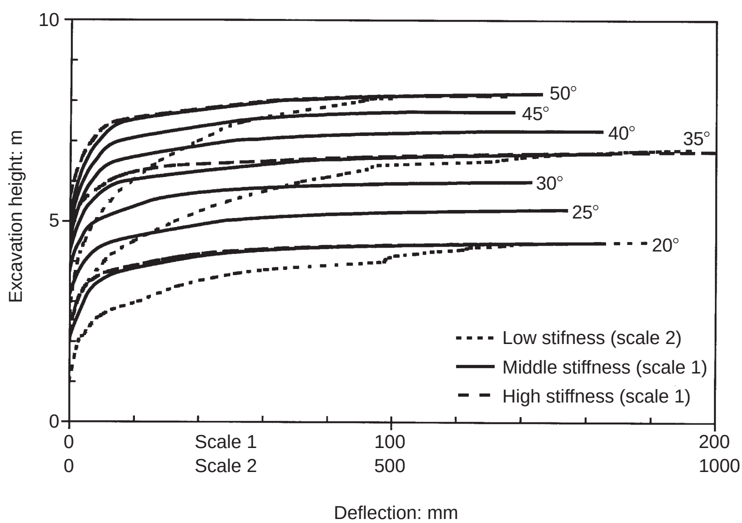

Fig. 7. Deflection of top of wall

stress ($K_0 = 0{\cdot}5$). Analyses by Fourie & Potts (1989) and Day & Potts (1993) have shown that the initial value of K_0 does not affect the failure height of excavation. The analyses assume fully drained conditions with pore pressure equal to zero and are therefore applicable to the long-term condition. The Imperial College Finite Element Program was used for the analyses.

An elastic–perfectly plastic cohesionless Mohr–Coulomb model was used to describe the soil behaviour. A range of analyses was performed with the friction angle, ϕ', of the soil equal to 20°, 25°, 30°, 35°, 40°, 45° and 50°. In each case, the angle of dilation was taken as half the friction angle. The bulk unit weight of the soil, γ, equals $20\ kN/m^3$. The Young's modulus equals $5000 + 5000z$ kPa, where z is the depth measured from the original ground surface. The Poisson's ratio equals 0·2.

The wall was assumed to be elastic with properties equivalent to a reasonably stiff sheet pile: $E = 2{\cdot}1 \times 10^8$ kPa, $I = 46{\cdot}8 \times 10^{-4}\ m^4/m$ width, and $A = 5{\cdot}26 \times 10^{-2}\ m^2/m$. The wall was assumed to be rough in all analyses. For the cases of soil strength, $\phi' = 20°$, 35° and 50°, additional analyses were done using walls 100 times less stiff and 100 times more stiff in bending ($I = 46{\cdot}8 \times 10^{-6}\ m^4/m$, $A = 1{\cdot}13 \times 10^{-2}\ m^2/m$ and $I = 46{\cdot}8 \times 10^{-2}\ m^4/m$, $A = 24{\cdot}4 \times 10^{-2}\ m^2/m$).

ANALYSIS OF RESULTS

The net horizontal earth pressure on the wall obtained from the finite element analyses at limiting equilibrium at the integration points is shown in Figs 8–12 for the analyses using $\phi' = 20°$, 25°, 35°, 40° and 50°. The upper 4 m of the wall, on which the pressure distribution is linear, has been omitted for clarity. The results of the other analyses are similar. For the cases of $\phi' = 20°$, 35° and 50°, the results of the analyses with different wall stiffness are similar to the results shown. The limiting equilibrium height of excavation is also marked on these figures by a horizontal line. This was taken as the last height at which numerical convergence was achieved and is estimated to have an accuracy of 0·1 m. The bending moment distributions in the wall for these analyses are shown in Figs 13–17. The results of the other analyses are similar.

Net pressure distribution

The integration point stress distributions indicate that the net pressure distribution is characterized by a linear part above the excavation level and a linear part immediately below the excavation level, extending almost to the point of the maximum value. Below the maximum, to the bottom of the wall the net pressure is non-linear. The wall stiffness has very little effect on the limiting equilibrium excavation height and the net pressure on the wall at failure.

The aim of the finite element analyses was to determine the validity of the assumptions used in the rectilinear net pressure method. Hence, the rectilinear pressure distribution shown in Fig. 3 was fitted to the net pressure data points (integration points) obtained from the finite element analyses. The best-fit line is plotted in Figs 8–12. The rectilinear best-fit approximation was found in the following way:

(*a*) Using a least squares fit to the bending

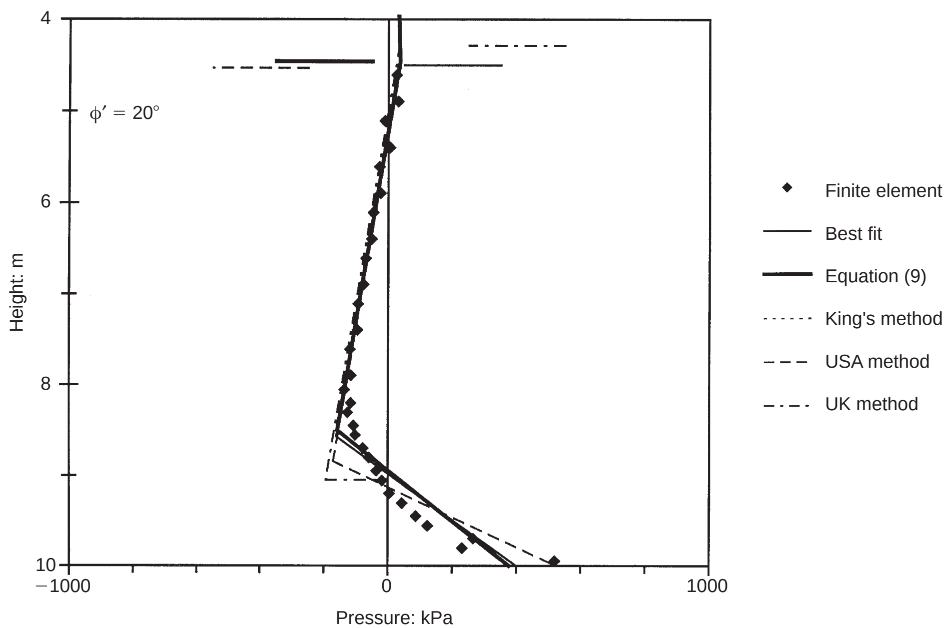

Fig. 8. Net pressure distribution – $\phi' = 20°$

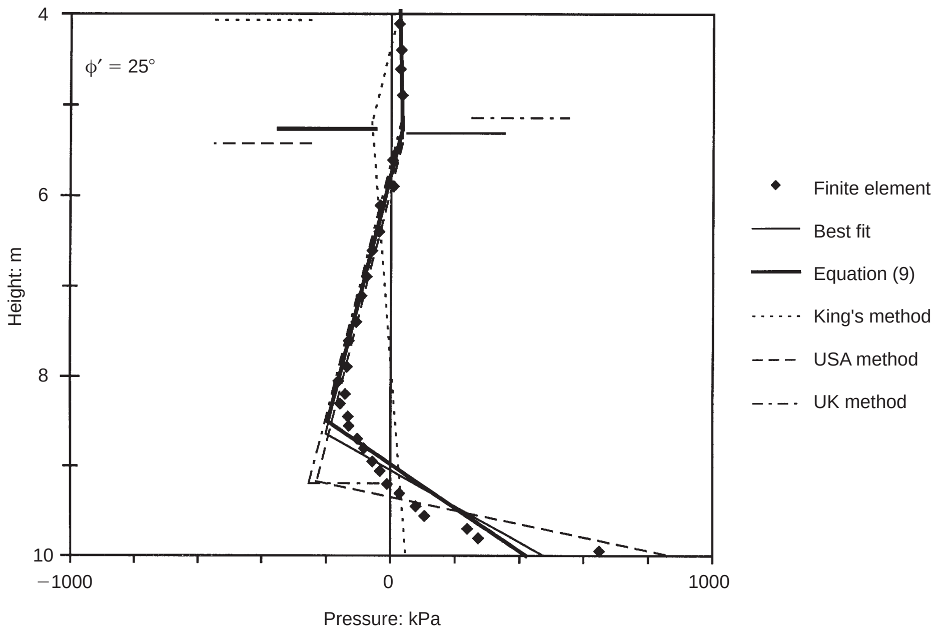

Fig. 9. Net pressure distribution – $\phi' = 25°$

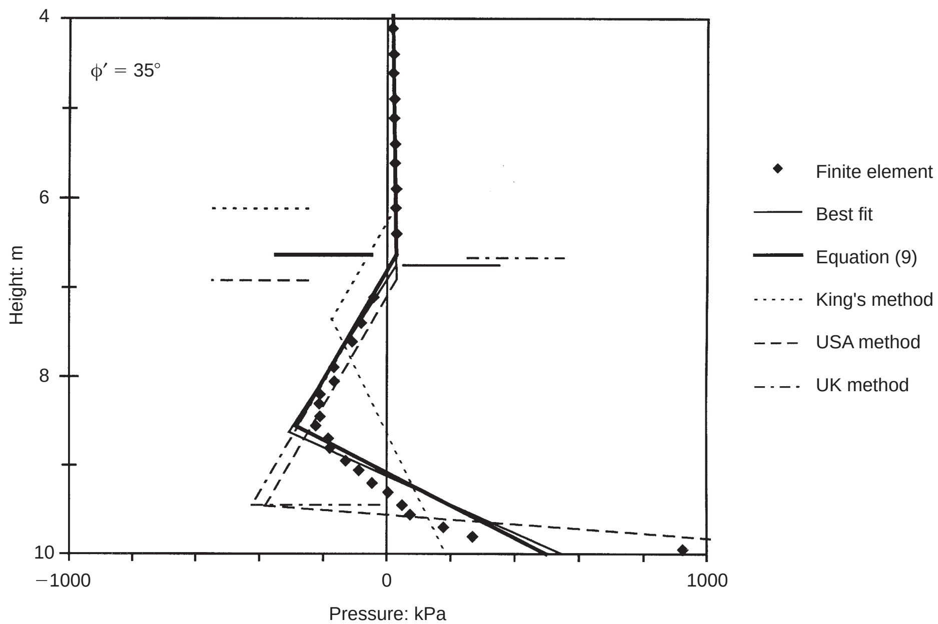

Fig. 10. Net pressure distribution – $\phi' = 35°$

moment data points above the excavation level, the value of p_a was determined. The bending moment was used instead of the stresses because the bending moment is very sensitive to small changes in the pressure.

(*b*) Using this value of p_a, the values of p_1, p_2 and y were determined by a least squares fit of the rectilinear pressure distribution to the finite element net pressure data points over the full wall length. The values of p_1, p_2 and y were

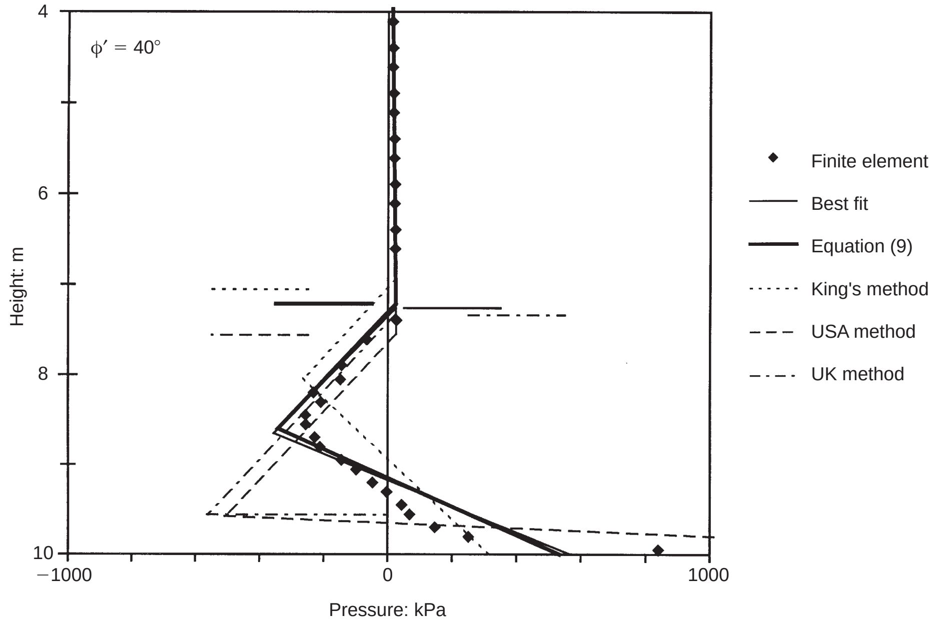

Fig. 11. Net pressure distribution – $\phi' = 40°$

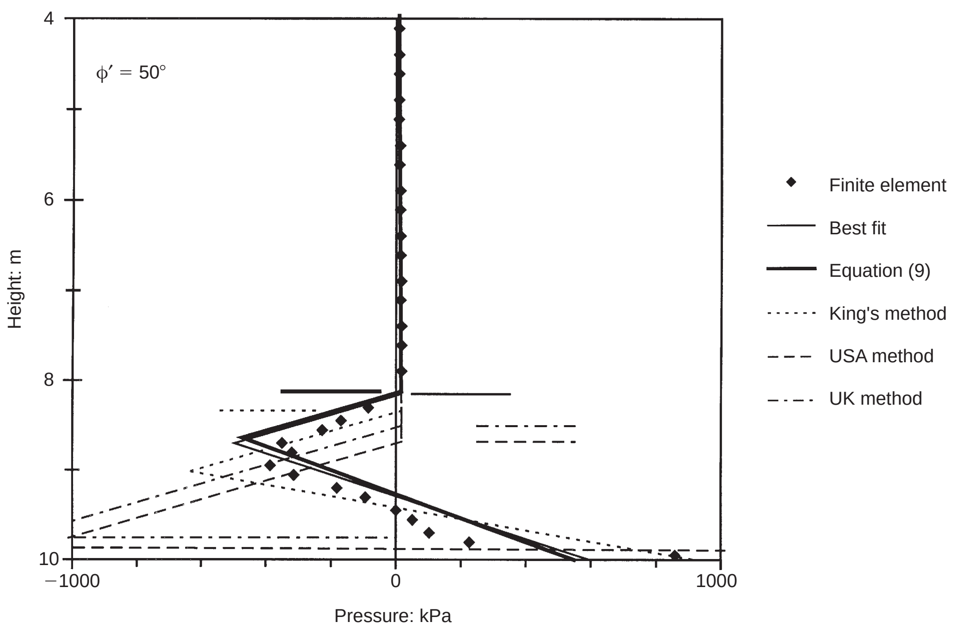

Fig. 12. Net pressure distribution – $\phi' = 50°$

additionally constrained so that the net horizontal force and net moment on the wall were zero. The resulting best-fit rectilinear net pressure distribution satisfies both moment and force equilibrium. It is a close approximation to the data points obtained from the finite element analyses.

Having determined the best-fit rectilinear pressure distribution, the following were determined from

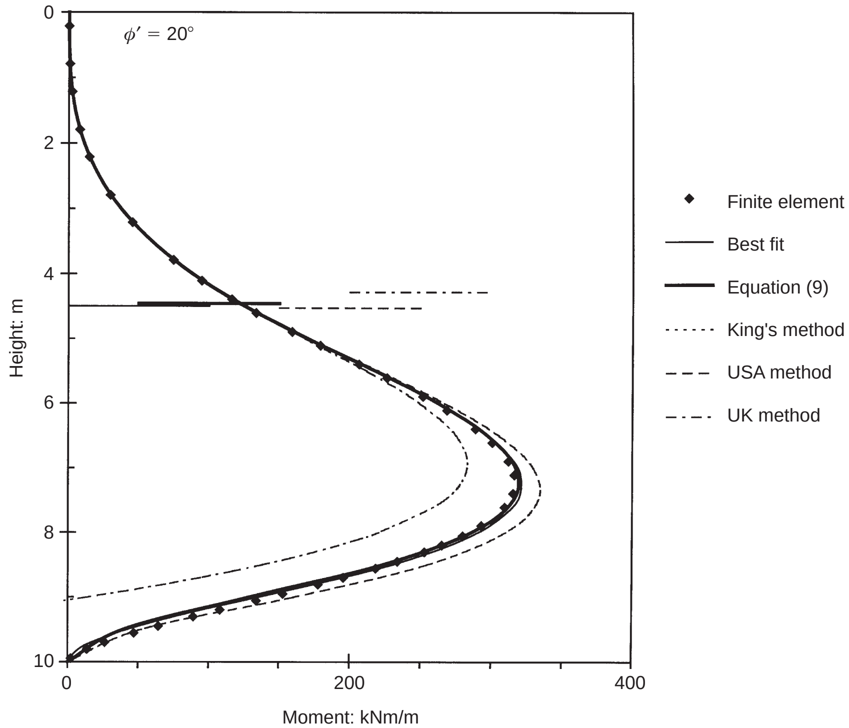

Fig. 13. Bending moment distribution – $\phi' = 20°$

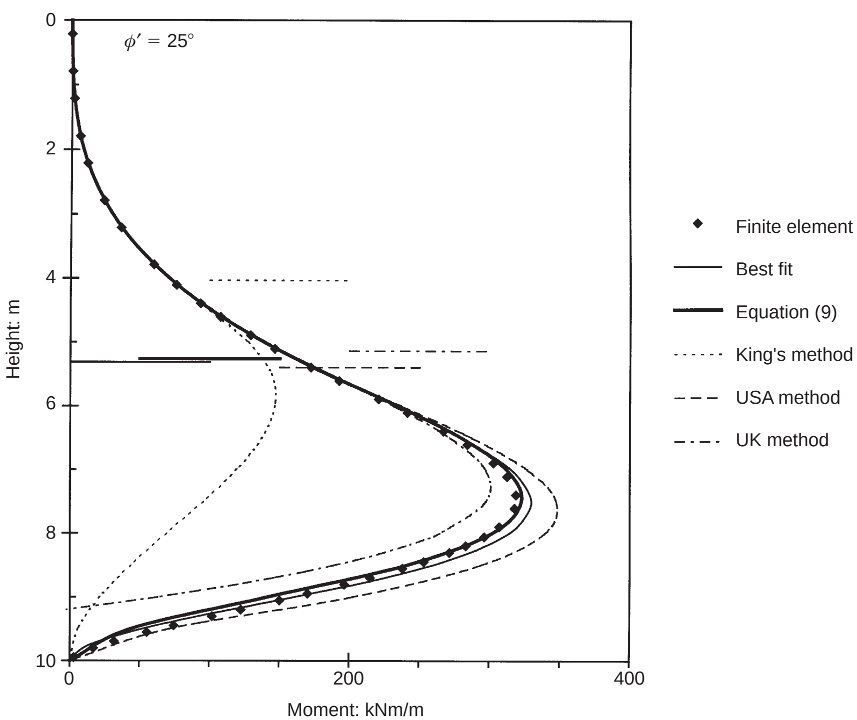

Fig. 14. Bending moment distribution – $\phi' = 25°$

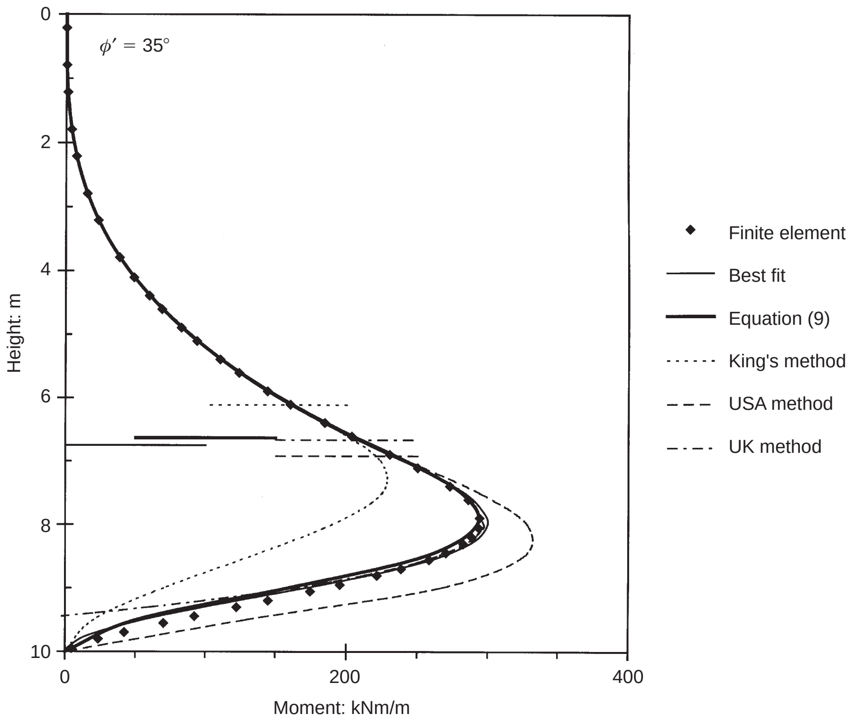

Fig. 15. Bending moment distribution – $\phi' = 35°$

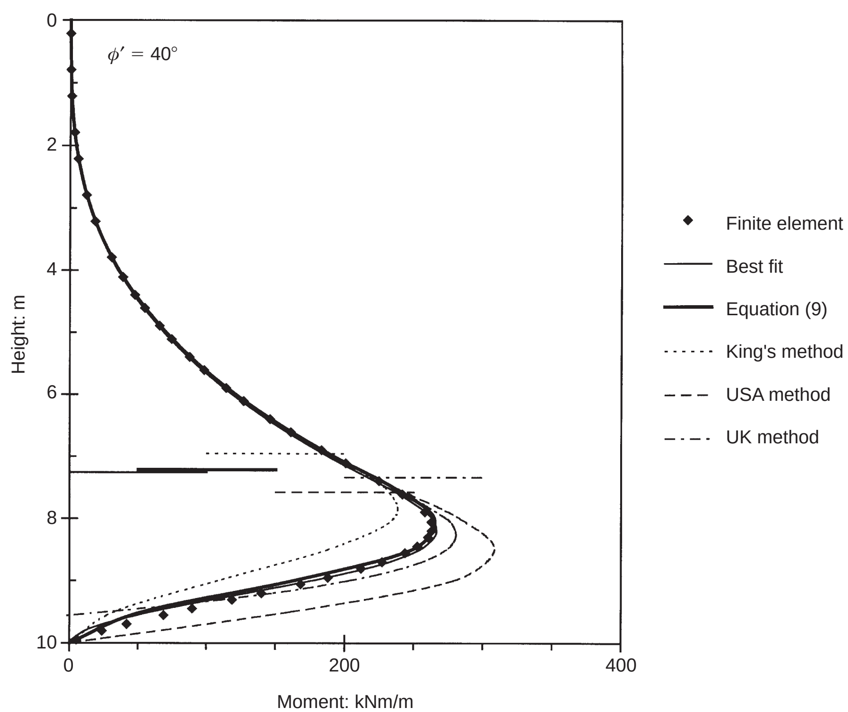

Fig. 16. Bending moment distribution – $\phi' = 40°$

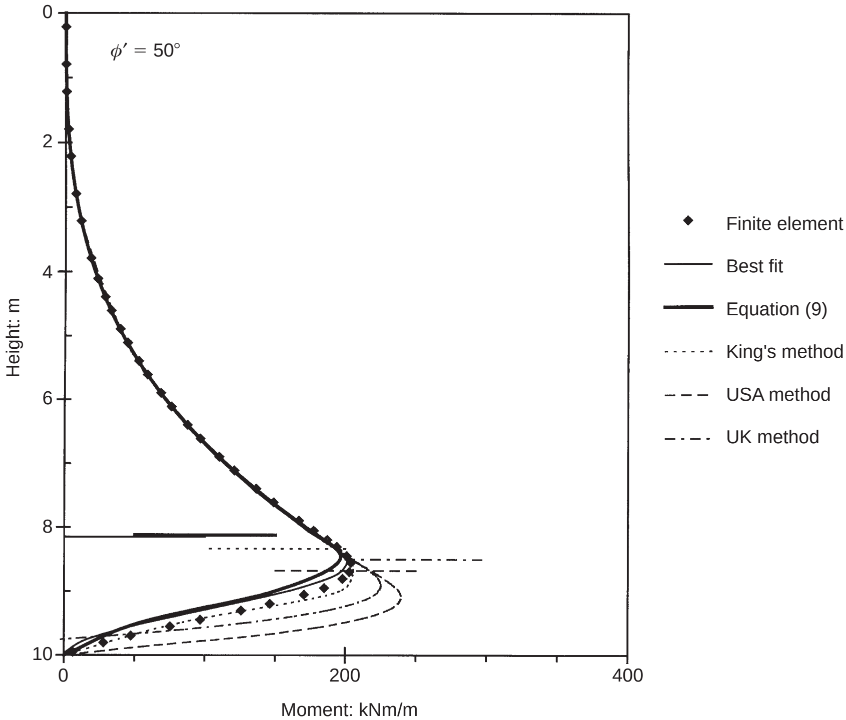

Fig. 17. Bending moment distribution – $\phi' = 50°$

the values of p_a, p_1, p_2, y and the wall geometry, h and d:

(*a*) The distance from the bottom of the wall of zero net pressure, ε'.
(*b*) The active pressure coefficient, K_a. In all cases, K_a was within 2% of the theoretical value given by Caquot & Kerisel (1948) for a rough wall.
(*c*) The passive pressure coefficient immediately below the excavation level, K_p, that is inferred from the rectilinear pressure distribution between p_a and p_1.

For comparison with the value of K_p inferred from the best-fit rectilinear pressure distribution (above), K_p was also determined from the finite element integration point stresses. This was calculated using a least squares fit to the linear part of the passive pressure distribution immediately below the excavation.

The values of ε' determined in this manner are plotted against K_p/K_a in Fig. 18 for K_p determined in three different ways. The values of K_p used are the theoretical values given by Caquot & Kerisel (1948) for a rough wall, and those calculated by the two methods described above. It can be seen that there is very little difference between the different methods. Therefore, the theoretical passive pressure is fully mobilized below the excavation level and the first assumption used in the rectilinear net pressure method is quite reasonable. Also plotted on this diagram are the values of ε' that result from the assumptions used to define the net pressure distribution in the USA method.

Clearly, ε' is not constant and varies with respect to the limiting earth pressures (K_p/K_a). A good approximation to the actual value is given by equation (9), which is plotted on Fig. 18:

$$\varepsilon' = 0{\cdot}047 \ln\left(\frac{K_p}{K_a}\right) + 0{\cdot}1 \qquad (9)$$

The net pressure distribution and the predicted limiting equilibrium height of excavation given by the UK method, USA method, King's recommendation ($\varepsilon' = 0{\cdot}35$) and equation (9), in conjunction with theoretical pressure coefficients K_a and K_p given by Caquot & Kerisel (1948), are also plotted on Figs 8–12. This is akin to a design procedure. It is noted that King's assumption does not yield a solution in the case of $\phi' = 20°$, because K_p/K_a is less than 7·9. There is good agreement between the results based on equation (9) and the finite element

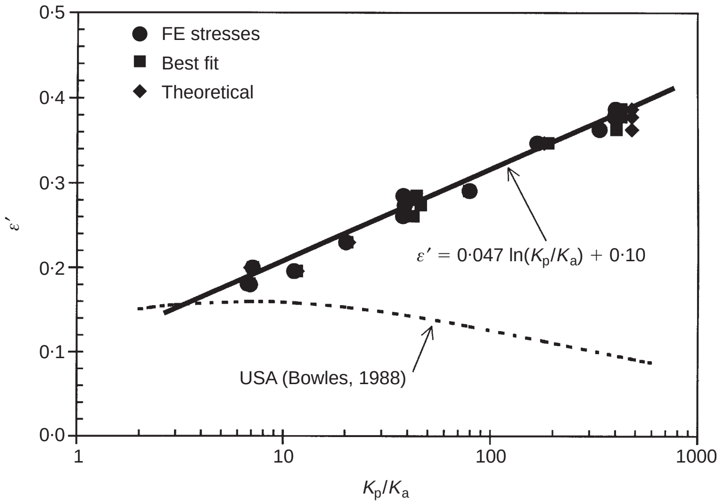

Fig. 18. Position of zero net pressure

results. Neither the USA method nor the assumption that $\varepsilon' = 0{\cdot}35$ produces good estimates of the limiting equilibrium height and net earth pressure over the full range of soil properties and wall friction. The USA method is reasonably good for low values of K_p/K_a, and King's assumption is reasonable at high values. Consequently, the USA method and the $\varepsilon' = 0{\cdot}35$ assumption produce erroneous bending moment distributions compared with the finite element results.

Bending moment at limiting equilibrium

In Figs 13–17 the bending moments calculated from the best-fit rectilinear net pressure are plotted. The best-fit rectilinear net pressure diagram produces a bending moment that is surprisingly close to the finite element bending moment. The bending moment obtained from the USA method, King's assumption ($\varepsilon' = 0{\cdot}35$), equation (9) and the UK method in conjunction with theoretical values of K_a and K_p are also shown.

Comparison of methods

The limiting equilibrium retained height obtained from the finite element analysis is the last stable height for which a numerical solution was obtained. It is estimated that the actual critical height is up to 0·1 m greater. The consequential range in h'_c is plotted in Fig. 19 against the ratio K_p/K_a. The values of K_a and K_p used here were determined from the integration point stresses in the soil immediately adjacent to the wall (as described above). Also plotted are the results of centrifuge tests reported by King (1995). The centrifuge experiments were performed by excavation of 0·5 m of soil at each stage (the wall was 11 m long). The actual limiting equilibrium height may therefore be up to 0·5 m greater than the last observed stable height, which is reported by King. This range is plotted in Fig. 19. There is excellent agreement between the finite element results and the centrifuge data. The limiting equilibrium height predicted by the rectilinear pressure distribution based on the assumptions that passive pressure is fully mobilized immediately below excavation and ε' is given by equation (9) is also plotted in Fig. 19. This method provides an excellent prediction of the finite element results and the centrifuge data over the full range of K_p/K_a.

The predictions of critical retained height and bending moment distribution by the USA and UK methods are reasonable at low values of K_p/K_a but not at high values. The assumption of $\varepsilon' = 0{\cdot}35$ is in better agreement with the data and finite element results at the upper values of K_p/K_a but appears very conservative at lower values.

CONCLUSION

A rectilinear net pressure distribution comprising three lines provides a good approximation to the actual net pressure distribution at limiting equilibrium. This distribution has the following characteristics:

(*a*) Active pressure is fully mobilized above the excavation level.
(*b*) Passive pressure is fully mobilized immediately below the excavation level.

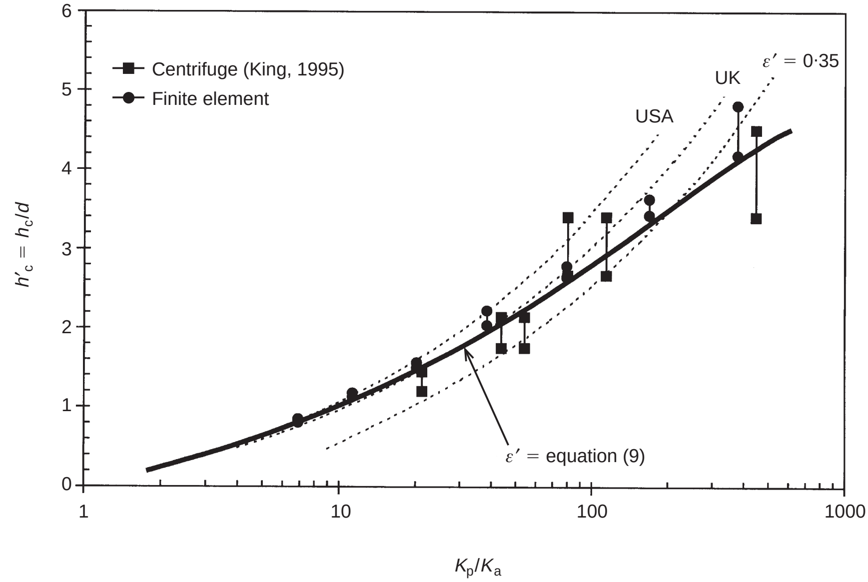

Fig. 19. Comparison of finite element results, centrifuge data and design methods

(*c*) The point of zero net pressure is dependent on the active and passive pressure coefficients and is defined by equation (9).

The limiting equilibrium retained height and the bending moment distribution predicted by this rectilinear net pressure are in excellent agreement with centrifuge data and finite element analyses over the full range of soil strength and wall friction coefficients.

The proposal by King (1995) that $\varepsilon' = 0{\cdot}35$ is generally conservative. The predicted limiting equilibrium retained height and maximum bending moment are generally less than is indicated by the finite element data. This is particularly so where the value of K_p/K_a is low. In some cases, such as low-strength soil and/or frictionless wall, the assumption that $\varepsilon' = 0{\cdot}35$ will not yield a solution where one is clearly physically possible.

Equation (9), the rectilinear net pressure distribution and pressure coefficients given by Caquot & Kerisel (1948), may be used as a design method to predict the limiting equilibrium retained height and bending moment distribution. Such predictions will be more accurate than existing design methods commonly used in the UK and USA.

These recommendations allow accurate calculation of the limiting equilibrium or limit state situation. For safety and serviceability, the depth of excavation will, of course, be less than the limiting value. Further investigation is required to determine whether a rectilinear pressure distribution may be as good an approximation to the net pressure in the realistic situations when the retained height is less than the limit state value. The *in situ* stress (K_0) and wall stiffness are likely to be more significant in this situation.

REFERENCES

Bica, A. V. D. & Clayton, C. R. I. (1989). Limit equilibrium design methods for free embedded cantilever walls in granular materials. *Proc. Instn Civ. Engrs Part 1* **86**, 879–989.

Bica, A. V. D. & Clayton, C. R. I. (1993). The preliminary design of free embedded cantilever walls in granular soil. In *Retaining structures* (ed. C. R. I. Clayton), pp. 731–740. London: Thomas Telford.

Bowles, J. E. (1988). *Foundation analysis and design*, 4th edn. New York: McGraw-Hill.

Bransby, J. E. & Milligan, G. W. E. (1975). Soil deformations near cantilever retaining walls. *Géotechnique* **24**, No. 2, 175–195.

Caquot, A. & Kerisel, J. (1948). *Tables for the calculation of passive pressure, active pressure and bearing pressure of foundations*. Paris: Gauthier-Villars.

Day, R. A. & Potts, D. M. (1993). Modelling sheet pile retaining walls. *Computers Geotechnics* **15**, 125–143.

Fourie, A. B. & Potts, D. M. (1989). Comparison of finite element and limiting equilibrium analyses for an embedded cantilever wall. *Géotechnique* **39**, No. 2, 175–188.

King, G. J. W. (1995). Analysis of cantilever sheet-pile walls in cohesionless soil. *J. Geotech. Engng Div., ASCE* **121**, No. 9, 629–635.

Lyndon, A. & Pearson, R. A. (1985). Pressure distribution on a rigid retaining wall in cohesionless material. *Proceedings of international symposium on application of centrifuge modelling to geomechanics design* (ed. W. H. Craig), pp. 271–280. Rotterdam: Balkema.

Padfield, C. J. & Mair, R. J. (1984). *Design of retaining walls embedded in stiff clays*, Report 104. London: Construction Industry Research and Information Association.

Rowe, P. W. (1951). Cantilever sheet piling in cohesionless soil. *Engineering* September 7, 316–319.